Chapter 5

Current-Controlled SRM Fed by Three-Phase Boost PFC

Erdal Şehirli and Meral Altınay

Additional information is available at the end of the chapter

http://dx.doi.org/10.5772/intechopen.69150

Abstract

In this chapter, firstly, converter types of switched reluctance motor (SRM) are described. Current control structure of SRM, which has six stator and four rotor poles, over an asymmetric bridge converter, is also explained. While feeding SRM by an AC grid, grid voltages have to be converted to DC voltage; to realize this conversion, in order to obtain high power factor and sinusoidal grid current, power factor correction (PFC) circuits must be used. In this study, an asymmetric bridge converter of SRM is fed by three-phase PFC boost converter that consists of uncontrolled diode rectifier and DC-DC boost converter with high frequency operation. PFC boost converter is controlled by nonlinear control algorithm. By means of the simulations that are conducted by MATLAB/Simulink, grid voltage and current, current harmonics of each phase, three-phase currents of phases, flux, and current of SRM are presented. Simulation results show that proposed SRM that is fed by three-phase PFC boost converter system gives the desired performance, for both grid and SRM side.

Keywords: converter, PFC, current control, SRM

1. Introduction

Recently, using SRM has taken much attention because of improving semiconductor and microprocessor technology. Furthermore, SRM has some advantages that are having concentric stator winding and salient stator, rotor poles without any winding, and magnets. Besides, with respect to induction motor drivers, SRM driver needs lesser switch. Another advantage of SRM is to have constant torque characteristic. On the other hand, one of the important disadvantages of SRM is torque ripple. But torque ripple can be improved with converter types.

SRM is not operated by using only DC source. To drive SRM, converter topologies such as asymmetric bridge, r dump, c dump are required. Furthermore, SRM converter needs DC power to operate. This DC power can easily be obtained by using an AC grid that can be single- or three-phase over rectifiers. However, if the AC grid is converted to DC by uncontrolled rectifiers, grid current has harmonics and the power factor of AC grid decreases. To overcome these problems, improved power quality converter that contains pulse width modulated (PWM) rectifiers and power factor correction (PFC) circuits should be used.

In literature, there are so many publications about SRM that are related with construction, operation, control, its converters, and obtaining a high power factor while feeding SRM. Some of the publications are summarized as follows.

In Refs. [1, 2], fundamental information about control, design, operation, and converter types of SRM is given. Converter and driver types for SRM are also expressed and compared [3, 4]. Studies on control of SRM that are about speed, torque, and current control are implemented [5–9]. Control topologies, such as adaptive, fuzzy, sliding, and nonlinear are realized for SRM [10–12].

Some new applications of SRM that are battery chargers, water pumping systems, electrical vehicles, and solar photo voltaic (PV)-powered drives are explained [13–16].

Krishnan and Lee [17] implement C dump converter with four-phase SRM, and Consoli et al. [18] is for three-phase SRM that is fed by single-phase PFC boost converter, and they provide higher power factor. Single-phase half-controlled PWM boost converter-based PFC converter is used for feeding four phases of SRM that is driven by an asymmetric bridge converter as in Ref. [19] in order to obtain high power factor, and it has DC-DC converter between PFC converter and asymmetric bridge converter. Another application that obtains a high power factor, with asymmetric bridge converter, is realized for four phases of SRM by using single-phase PFC boost converter [20]. Reinert and Schroder [21] emphasize the need of PFC circuit for SRM by pointing out single-phase boost PFC and asymmetric bridge converter. Single-phase PFC boost converter is included with hysteresis current-controlled SRM drive [22], and the same study with fuzzy tuned proportional-integral-derivative (PID) controller for PFC converter is made in Ref. [23]. Rajesh and Singh [24] present SRM with midpoint converter that is fed by Vienna rectifier for having higher power factor. SRM is also driven by midpoint converter and fed by single-phase three-level rectifier as a PFC circuit [25]. To have reversible power flow and regenerative specification [26], two different PFC converters that are active power filters (APC) and three-phase voltage sourced converters (VSC) are implemented. Power quality is improved by using Zeta converter [27] and canonical switching cell converter [28] for midpoint converter-driven SRM.

In this chapter, converter types of SRM are described. Current control structure of SRM which has six stator and four rotor poles, over asymmetric bridge converter, is also explained. Furthermore, in this study, asymmetric bridge converter of SRM is fed by three-phase PFC boost converter that consists of uncontrolled diode rectifier and DC-DC boost converter with high frequency operation. PFC boost converter is controlled by nonlinear control algorithm. By means of the simulations that are conducted by MATLAB/Simulink, grid voltage and current, current harmonics of each phase, three-phase currents of phases, flux, and current of SRM are presented. Simulation results show that proposed SRM that is fed by three-phase PFC boost converter system gives the desired performance, both grid and SRM side.

2. Converter types for SRM

SRM is not operated without using converter topologies. In literature, SRM converters are classified as shown in **Figure 1** [1]. This classification is based on the switch number in converter topology.

Some of the converter topology from each classification, that are two-stage power converters, asymmetric bridges, R dump converter, and C dump converter, is expressed briefly as follows.

2.1. Two-stage converter

In a two-stage converter, power conversion is realized as bidirectional that is transferring energy from SRM to grid and from grid to SRM. The block diagram of two-stage topology is shown in **Figure 2** [1]. In **Figure 2**, it has been shown that when the SRM is used as a generator, prime mover is attached to SRM and inverter is used to obtain three-phase voltage for grid integration. However, when the SRM is used as a motor, rectifier is used to feed SRM from the three-phase grid and load is replaced with prime mover.

2.2. 1.5 switch/phase converter

1.5 q converter that is shown in **Figure 3** [1] is just suitable for SRM that has even number of phases. Energizing for each phase, 1.5 switch and diodes are required. The operation of 1.5 switch converter is described as follows. To energize phase a, S_1 and S_5 is turned on, while S_3 and S_6 is turned off. At that time, phase c current freewheels over D_5. After that, for energizing phase b, S_2 and S_6 have to be turned on when S_5 has to be turned off and current of phase a flows from S_1 to D_5. Then, phase c should be energized by turning on S_3 and S_5 while turning off S_6 and S_1. Furthermore, phase b current flows from S_2 to D_6 and phase a current freewheels

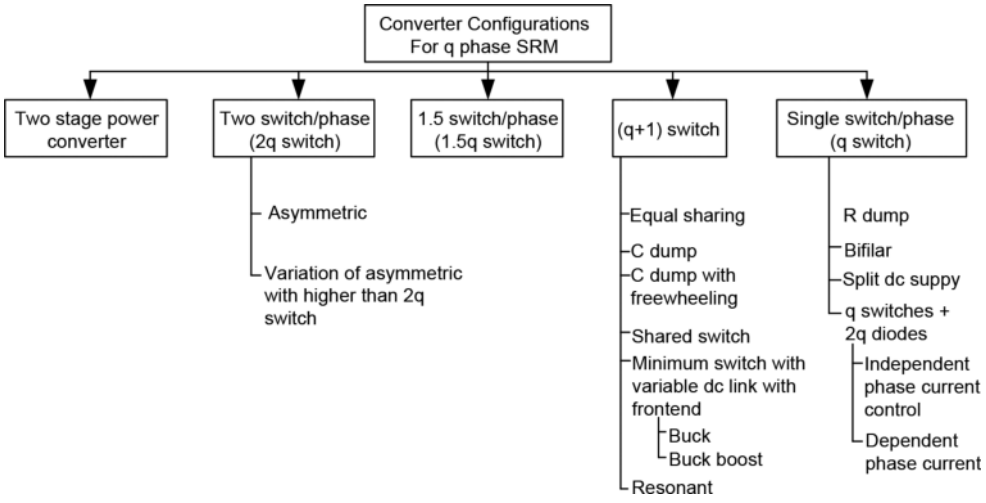

Figure 1. The converter classification of SRM [1].

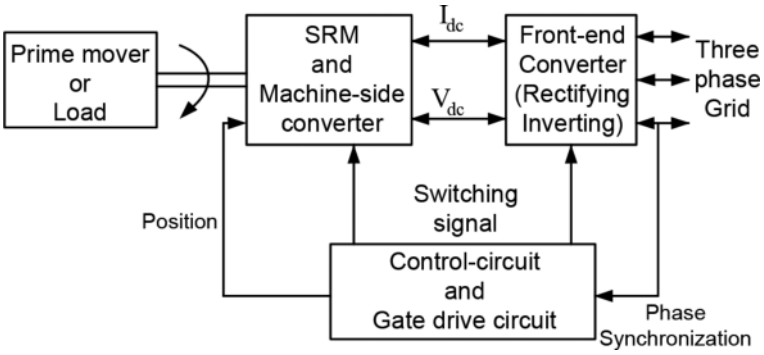

Figure 2. A block diagram of a two-stage converter.

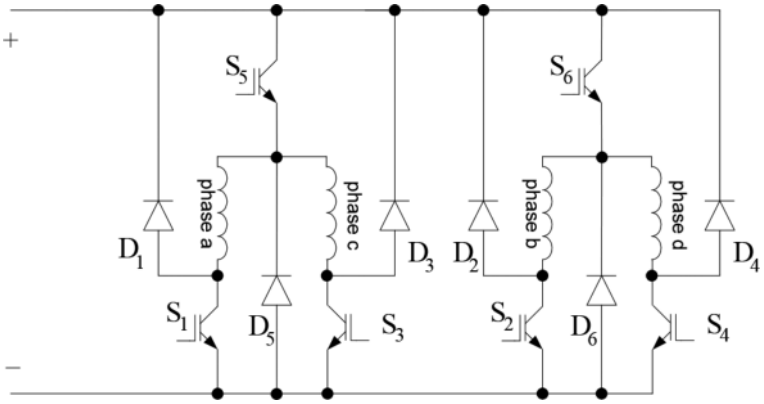

Figure 3. 1.5 switch/phase converter.

over D_1. At last, to energize phase d, S_6 and S_4 should be turned on after turning off S_5 and S_2. Besides, phase c current flows from S_3 to D_5, while phase b current freewheels over D_2.

2.3. R dump converter

R dump converter is shown in **Figure 4**. Operation of R dump converter can be summarized as follows. After each power switch turns off, current passes through the diodes and charge C; then, current flows through R and resets the energy in phase windings.

Due to the use of R for extinguishing energy of phase windings, energy is dissipated and overall efficiency reduces.

2.4. C dump converter

Figure 5 shows a C dump converter. In C dump converter, energy recovery process is being done by S_4, D_4, L, and C. Operation is briefly as follows: firstly the energy of phase windings is

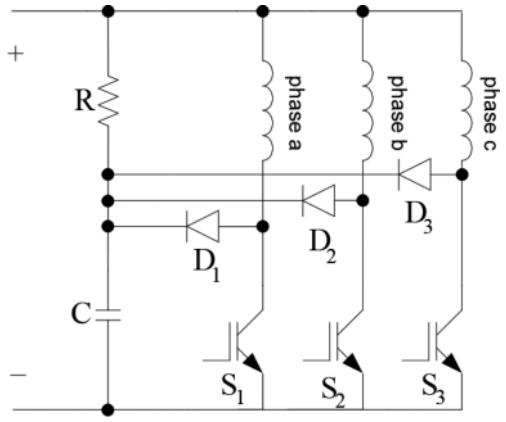

Figure 4. R dump converter of SRM.

stored on C and then by switching on S_4, stored energy on C is sent to DC source or phase windings over L and D [1, 29].

2.5. Asymmetric bridge converter

In asymmetric bridge converter that is shown in **Figure 6**, for each phase of SRM, there are two power switches and two diodes.

The sample connection of switches and diodes to one phase of SRM is shown in **Figure 7**. It is also seen from the same figure that SRM has six stator and four rotor poles. It is the same structure as the study that is carried out in this chapter.

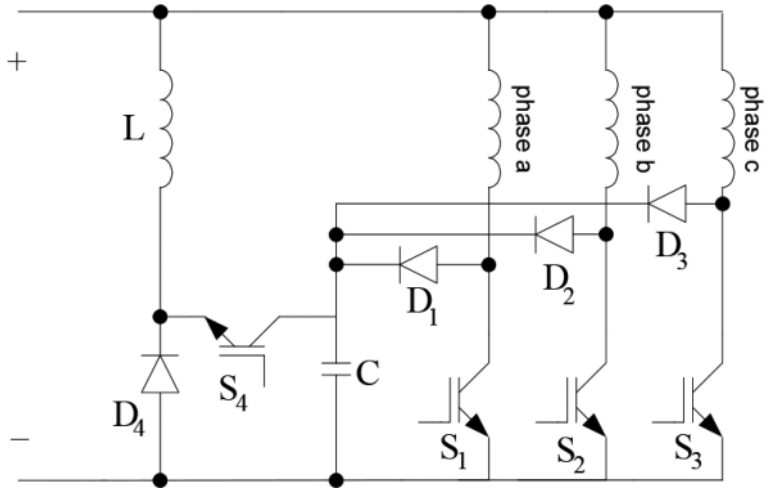

Figure 5. C dump converter of SRM.

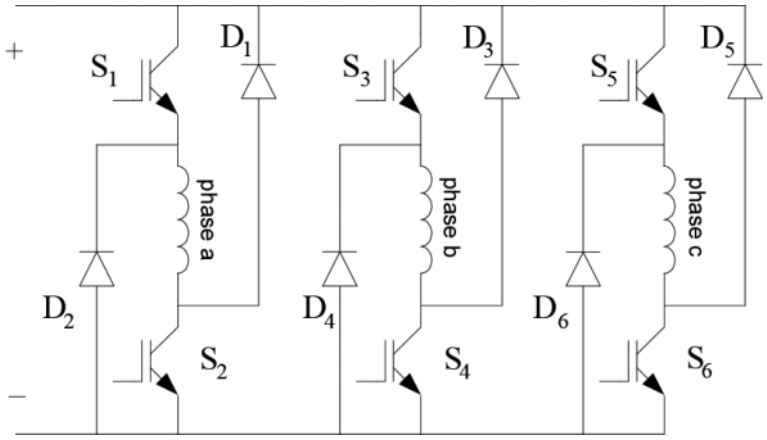

Figure 6. Asymmetric bridge converter of SRM.

Basically, the definition of **Figure 7** and the operation of asymmetric bridges are as follows: windings are placed mutually on stator poles and they are connected in series to compose N and S poles. After energizing phase one winding with S_1 and S_2 switches, current flows from DC power supply to phase winding. When switches turn off, current flows through D_1 and D_2 diodes and negative voltage is applied to phase winding that causes decreasing of winding current. So, energy turns back to power supply [30].

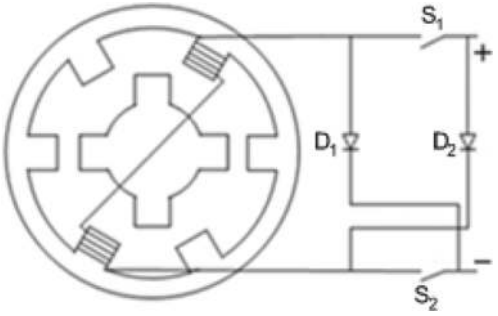

Figure 7. Connection of an asymmetric bridge to SRM.

3. Current control of SRM

In literature, in order to control speed of SRM, current control of SRM has to be done as a first stage that is seen in generalized speed control block diagram in **Figure 8**.

Furthermore, current control of SRM can be realized by hysteresis and PWM methods [30]. In this chapter, PWM-based control is chosen as a current controller. In **Figure 9**, current control block diagram is shown.

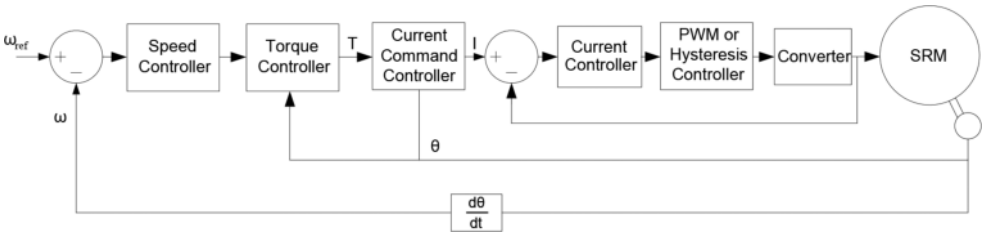

Figure 8. A generalized speed control block diagram of SRM.

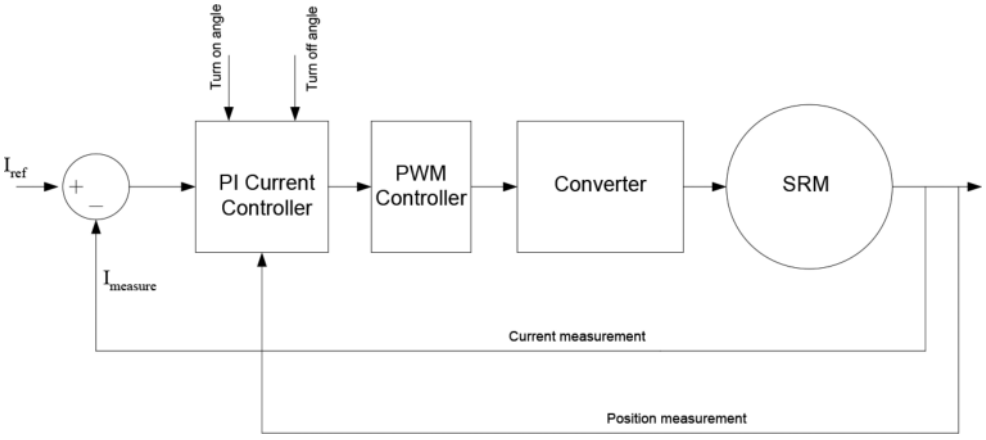

Figure 9. Current control block diagram of SRM.

In **Figure 9**, it is seen that, winding currents of SRM are measured and compared with the reference current. After current comparison, current differences are sent to PI current controller block. PI current controller block produces appropriate control signals with respect to turn-on and turn-off angle of SRM's rotor position. Then, these signals are applied to PWM block in order to obtain gating pulses of the asymmetric bridge converter. After applying pulses to asymmetric bridge converter, SRM is driven [30].

4. Three-phase PFC boost converter

SRM can be fed after rectifying the AC grid. This rectification process can be done by using wide variety of rectifiers that are conventional rectifiers and increased power factor corrected converters. In **Figure 10**, all the converters that are in literature [31] are classified.

However, conventional rectifiers that use uncontrolled and controlled thyristors do not provide a high power factor and sinusoidal grid currents. So, with conventional topologies, AC grid is not used efficiently. Therefore, in order to obtain high power factor and sinusoidal grid

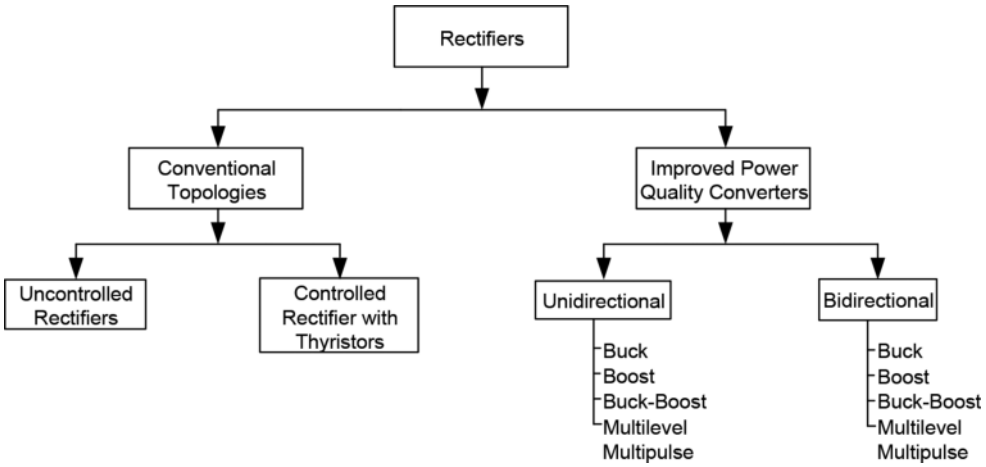

Figure 10. Classification of converters that can be used as front-end converter for SRM.

currents, increased power factor correction topologies (IPQC) are chosen. IPQC topologies can also be classified with respect to the power flow as unipolar and bipolar topologies [31].

By using the bipolar topologies, SRM can also be operated as a motor and generator, or regenerative operation of SRM is provided. But bipolar topologies include many power switches. So, it increases the cost of the converter. On the other hand, unipolar topologies include less power switch and the cost can be minimized. Also, implementation of unipolar converters is not as complex as bipolar converters.

In literature, some special properties of unipolar converters are generally called as PFC converters [32]. Furthermore, PFC converters can be realized by using any DC-DC converter, such as buck, boost, and buck-boost that are connected to the output of uncontrolled rectifier. This rectifier can be single or three phase. By operating the switch of DC-DC converter with the right control algorithm, a high power factor with sinusoidal grid current is obtained.

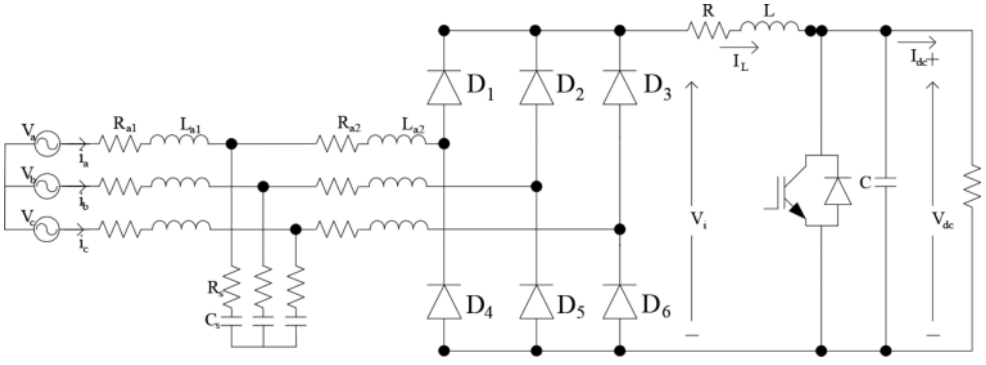

Figure 11. A three-phase PFC boost converter.

In **Figure 11**, three-phase PFC boost converter that has six diodes and one power switch is shown. It is seen in **Figure 11** that three-phase PFC boost converter is connected to the grid over inductor-capacitor-inductor (LCL) filter. In the LCL filter, series resistors to capacitors are connected in order to provide damping, and series resistor is used to show internal resistors of inductances.

A mathematical model of three-phase PFC boost converter can be written in Eq. (1) by applying Kirchhoff's current and voltage law with respect to the on and off position of the switch [32].

$$\begin{bmatrix} \dot{i_L} \\ \dot{V_{\mathrm{dc}}} \end{bmatrix} = \begin{bmatrix} 0 & (-1+\mathrm{d})/\mathrm{L} \\ (1-\mathrm{d})/\mathrm{C} & -1/\mathrm{RC} \end{bmatrix} \begin{bmatrix} i_L \\ V_{\mathrm{dc}} \end{bmatrix} + \begin{bmatrix} 1/\mathrm{L} \\ 0 \end{bmatrix} V_i \tag{1}$$

After applying nonlinear control method that is defined in Refs. [32–34], nonlinear controller for three-phase PFC boost converter is obtained in order to regulate DC voltage of the asymmetric bridge converter of SRM.

In **Figure 12**, nonlinear controller of three-phase PFC boost converter is shown as a block diagram.

Nonlinear controller in **Figure 12** needs to have reference current (I_{ref}), measured voltage (V_{dc}), and inductor current (I_L). Furthermore, reference current (I_{ref}) is produced by PI controller after comparing the square of reference and measured voltage [35]. Then, nonlinear control law is applied inside of nonlinear PFC controller block [30, 32]. After that, a new control variable (u) is obtained. By means of the comparison between u and a saw tooth wave form that has 100-kHz frequency in DC-PWM block, PWM pulse for power switch of PFC boost converter is acquired. After applying this PWM pulse to switch, required DC voltage is obtained.

In **Figure 13**, nonlinear controlled three-phase PFC boost converter is shown.

Nonlinear PFC controller for three-phase PFC boost converter is realized by using the Eq. (2) as in Refs. [30, 32–35].

$$\mathrm{u} = -\mathrm{K}(V_{\mathrm{dc}} - V_{\mathrm{REF}})\frac{C}{I_L} + 1 - \frac{V_{\mathrm{dc}}}{RI_L} \tag{2}$$

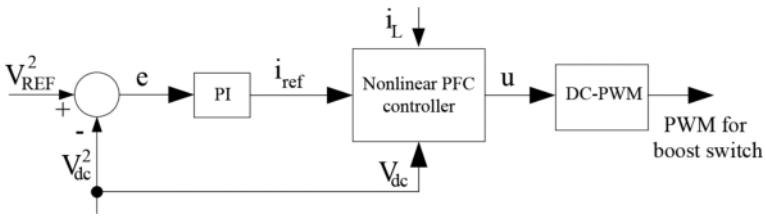

Figure 12. A block diagram of nonlinear controller of PFC boost converter.

5. Simulations

Current-controlled SRM that is fed by three-phase PFC boost converter is realized by simulation. In this simulation, Matlab/Simulink is used as in Refs. [36, 37]. A block diagram of simulation is shown in **Figure 14**.

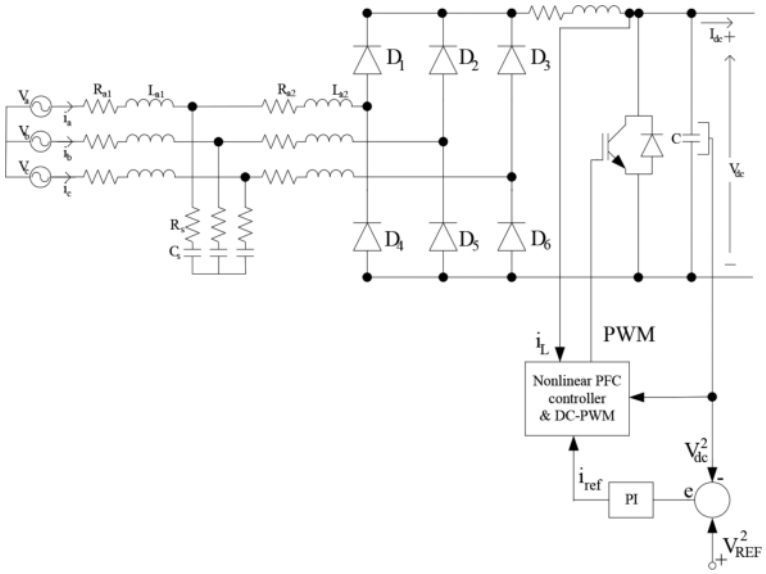

Figure 13. A block diagram of nonlinear controlled three-phase PFC boost converter.

In **Figure 14**, a three-phase AC grid is rectified by three-phase uncontrolled rectifier that is connected to grid by LCL filter. Besides, to build PFC structure, a boost converter that is operated with high switching frequency is added after the rectifier. PFC boost converter is controlled by nonlinear control structure and uses the DC-PWM technique to produce PWM pulse for power switch. Also, it is used to adjust the DC voltage of asymmetric bridge converter that is connected to SRM phase windings.

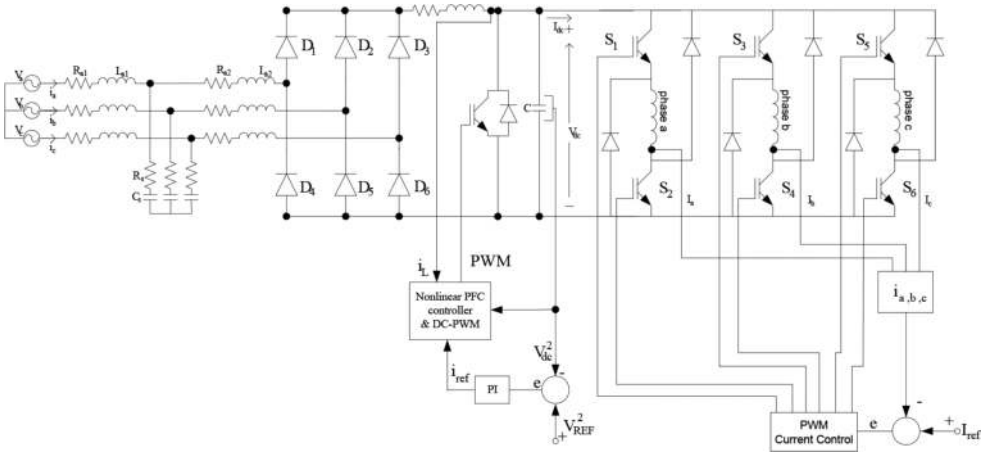

Figure 14. A block diagram of current-controlled SRM fed by three-phase PFC boost converter.

In **Figure 15**, simulation circuit is shown. In this simulation, SRM current and flux are measured with reference changes. Also, three-phase current and their harmonics, single-phase voltage, and current are shown. Furthermore, SRM is loaded with 10 Nm as a load.

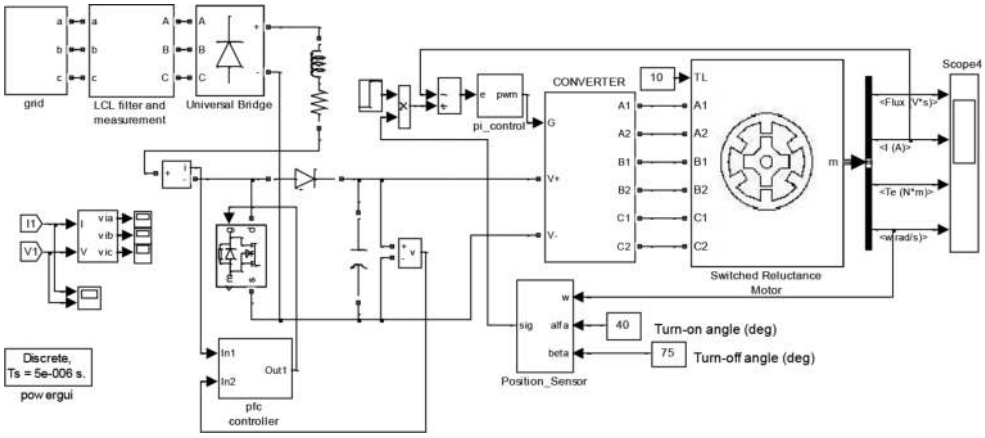

Figure 15. Simulation circuit of current-controlled SRM fed by three-phase PFC boost converter.

The parameters that are used in simulations are given in **Table 1**.

In **Figure 16**, SRM current is shown. In that figure, it is understood that SRM current reference is changed from 20 to 30 A at 0.5 s with maximum ±5 A ripple, and current is controlled as desired.

In **Figure 17**, SRM flux is shown under reference change of SRM current. After current reference increases, it is observed that flux increase as desired.

Passive components							
LCL filter						**DC link**	
R_{a1} (Ω)	L_{a1} (μH)	R_{a2} (Ω)	L_{a2} (H)	R_s (Ω)	C_a (F)	R_L (Ω)	C_{dc} (μF)
2	0.1	0.01	0.003	0.15	0.0023	1000	2200
SRM							
Poles		Stator resistance (Ω)	Inertia (kg.m)	Friction (Nms)	Current control	PI	
Stator 6	Rotor 4	0.05	0.05	0.02		K_p 5	K_i 10
Three-phase PFC boost controller							
DC link				Nonlinear controller			
K_p		K_i		K (10^9)			
1		10		1			
f (sw)	PFC boost	69 kHz		Asymmetric bridge		9 kHz	

Table 1. Parameters used in simulations.

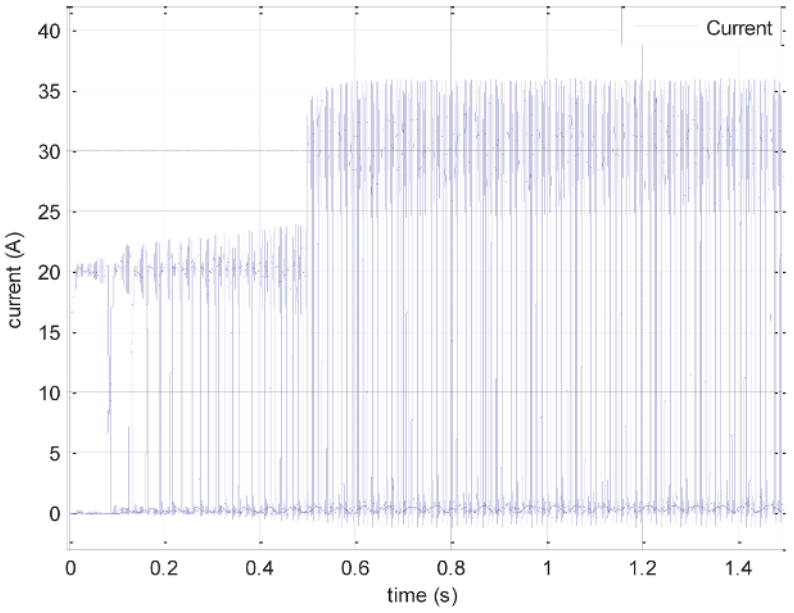

Figure 16. SRM current.

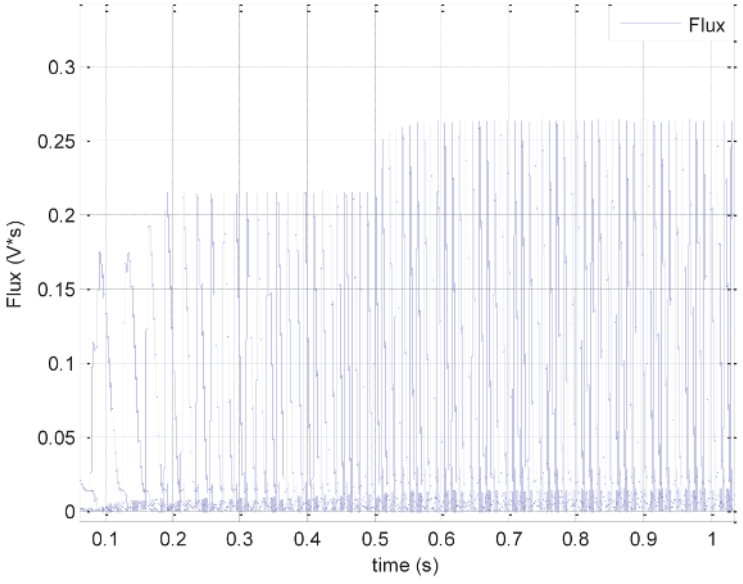

Figure 17. SRM flux.

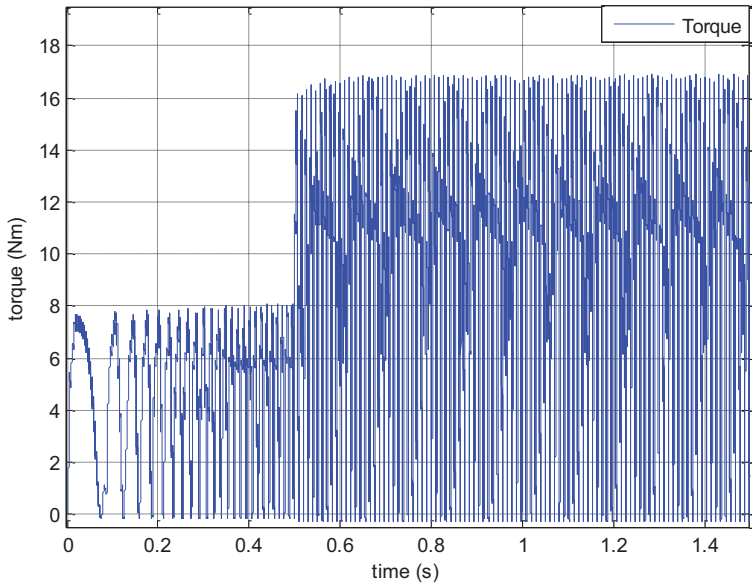

Figure 18. SRM torque.

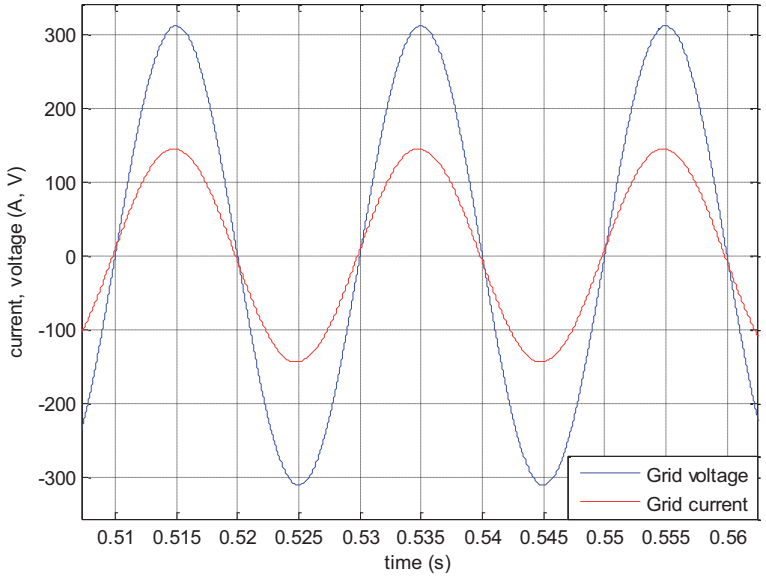

Figure 19. Single-phase current and voltage of grid.

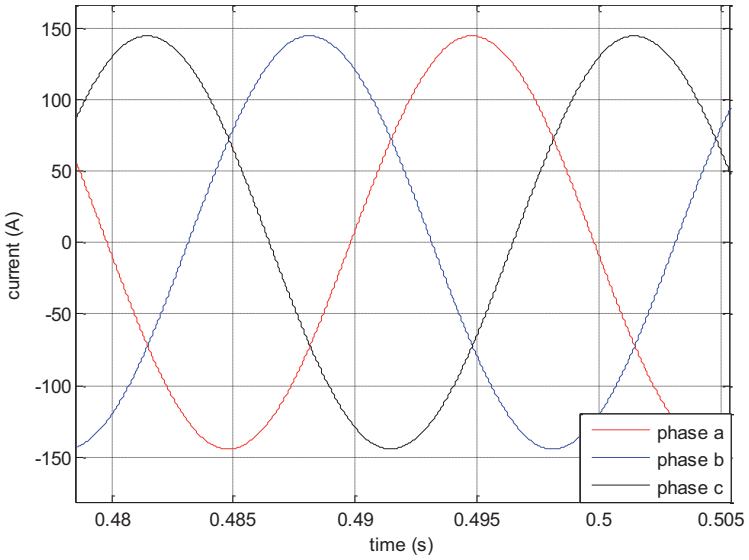

Figure 20. Three-phase currents of grid.

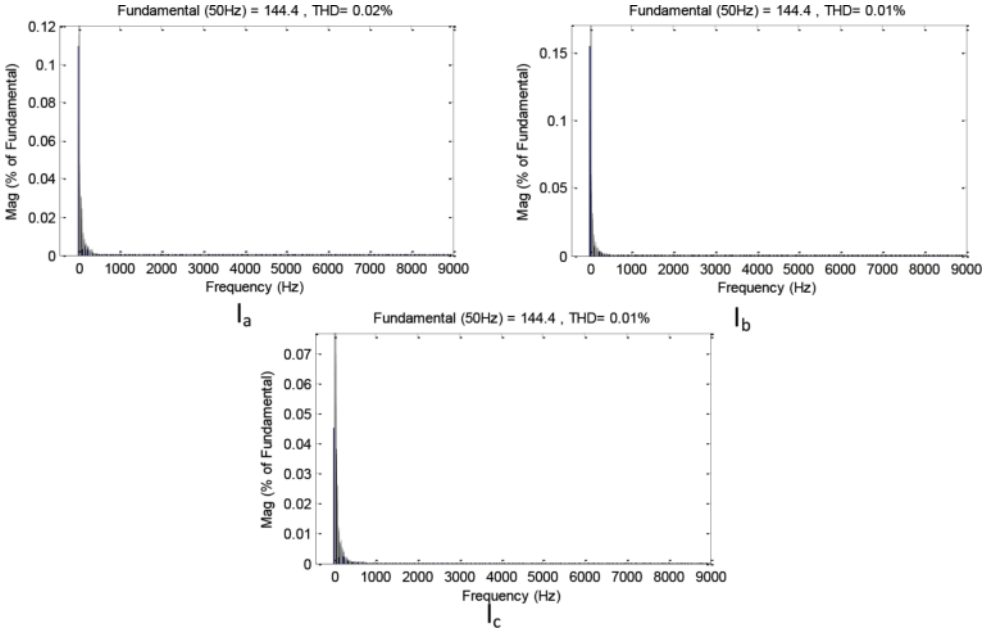

Figure 21. THDs of grid currents (Ia, Ib, Ic).

SRM torque per phase is shown in **Figure 18**. When current command is changed at 0.5 s, electromagnetic torque per phase of SRM is also changed.

Single-phase current and voltage are shown in **Figure 19**. It is observed that there is no phase shift between phase current and voltage. So, power factor is said to be unity. Therefore, there is no reactive power drawn from the grid.

In **Figure 20** three-phase currents are shown. It is seen that three-phase currents are sinusoidal and balanced.

Total harmonic distortion (THD)'s of three phase currents are shown in **Figure 21**. It is seen that THDs are 0.02, 0.01, and 0.01% for each phase, respectively. It can be understood by **Figures 19–21** that three-phase PFC boost converter operates as desired by providing DC power to SRM, lower THDs on grid current, and unity power factor.

6. Conclusion

In this chapter, firstly, SRM converter types that are commonly used such as asymmetric bridge, R dump, and C dump are expressed. Then, in order to supply DC power to SRM, rectifiers in literature are classified and three-phase PFC boost converter is chosen as a rectifier.

Furthermore, current-controlled SRM that is driven by using asymmetric bridge converter is realized while feeding SRM with three-phase PFC boost converter. Three-phase PFC boost converter is also controlled by a nonlinear method. This application is conducted over simulation which is realized with MATLAB/Simulink. By means of the simulation results, THDs of grid currents are obtained as 0.02, 0.01, and 0.01% for each phase, respectively. Also, grid voltage and grid currents are in the same phase so unity power factor is obtained. As a result, SRM current is controlled as desired as well.

Author details

Erdal Şehirli[1]* and Meral Altınay[2]

*Address all correspondence to: esehirli@kastamonu.edu.tr

1 Vocational School for Higher Education of Kastamonu University, Kastamonu, Turkey

2 Technology Faculty of Kocaeli University, Kocaeli, Turkey

References

[1] Krishnan R. Switched Reluctance Motor Drives. 1st ed. New Jersey: CRC Press; 2001

[2] Kuyumcu FE. Switched Reluctance Machine. 1st ed. Kocaeli: Lecture Notes; 2013

[3] Ha K, Lee C, Kim J, Krishnan R, Oh SG. Design and development of low cost and high efficiency variable speed drive system with switched reluctance motor. IEEE Transaction on Industrial Application. 2007;**43**(3):703–713. DOI: 10.1109/TIA.2007.895744

[4] Vukosavic S, Stefanovic VR. SRM inverter topologies: A comparative evaluation. IEEE Transaction on Industrial Application. 1991;**27**(6):1034–1047. DOI: 10.1109/28.108453

[5] Yuan G. Speed control of switched reluctance motors [thesis]. Hong Kong: The Hong Kong University of Science and Technology; 2000

[6] Bae HK. Control of switched reluctance motors considering mutual inductance [dissertation]. Virginia: Virginia Polytechnic Institute and State University; 2000

[7] Sahoo NC, Elamvazuthi I, Shaikh RA, Nor NM. A comparative study of Single Pulse Voltage and Hysteresis current control methods for switched reluctance motors. In: Energy, Automation, and Signal (ICEAS), 2011 International Conference on; 28–30 December; Bhubaneswar, Odisha, India: IEEE; 2011. p. 1–6. DOI: 10.1109/ICEAS.2011.6147145

[8] Maroon C, Garcia A, Tremps E, Somolinos JA. Torque control of switched reluctance motors. IEEE Transactions on Magnetics. 2012;**48**(4):1661–1664. DOI: 10.1109/TMAG.2011.2173169

[9] Deihimi A. Switched reluctance machine synthesis algorithms based on PWM control strategy for machine design optimization. In: 2008 11th International Conference on Optimization of Electrical and Electronic Equipment; 22–24 May; Brasov, Romania: IEEE; 2008. p. 51–56. DOI: 10.1109/OPTIM.2008.4602386

[10] Abut N, Cakir B, Inanc N, Yıldız AB, Bilgin MZ. Switched reluctance motor drive by using fuzzy controller. In: 23rd Industrial Electronic Control and Instrumentation. In: Industrial Electronics, Control and Instrumentation, 1997. IECON 97. 23rd International Conference on; 14 Nov.; New Orleans, LA, USA: IEEE; 1997. p. 348–353. DOI: 10.1109/IECON.1997.671075

[11] Amor LB, Dessaint LA, Akhrif O, Oliver G. Adaptive input output linearization of a switched reluctance motor for torque control. In: Industrial Electronics, Control, and Instrumentation, 1993. Proceedings of the IECON '93, International Conference on; 15–19 Nov.; Maui, HI, USA: IEEE; 1993. p. 2155–2160. DOI: 10.1109/IECON.1993.339410

[12] Li Y, Tang Y, Ji-bin C, Ai-hua L. Continuous sliding mode control and simulation of SRM. In: Cognitive Informatics & Cognitive Computing (ICCI*CC), 2011 10th IEEE International Conference on; 18–20 Aug.; Banff, AB, Canada: IEEE; 2011. p. 314–317. DOI: 10.1109/COGINF.2011.6016158

[13] Hu Y, Gan C, Cao W, Li C, Finney SJ Split converter-fed SRM drive for flexible charging in EV/HEV applications. IEEE Transaction on Industrial Electronics. 2015;**62**(10):6085–6095. DOI: 10.1109/TIE.2015.2426142

[14] Mishra KA, Singh B. SPV array powered zeta converter fed SRM drive for water pumping. In: 2015 IEEE Power, Communication and Information Technology Conference (PCITC); 15–17 Oct; Bhubaneswar, India. Bhubaneswar, India: IEEE; 2015. p. 476–482. DOI: 10.1109/PCITC.2015.7438213

[15] Gan C, Wu J, Yang S, Cao W, Guerroro JM. New integrated multilevel converter for switched reluctance motor drives in plug-in hybrid electric vehicles with flexible energy conversion. IEEE Transactions on Power Electronics. 2017;**32**(5):3754–3766. DOI: 10.1109/TPEL.2016.2583467

[16] Hu Y, Gan C, Cao W, Fang Y, Finney SJ. Solar PV-powered SRM drive for EVs with flexible energy control functions. IEEE Transactions on Industry Applications. 2016;**52** (4):3357-3366. DOI: 10.1109/TIA.2016.2533604

[17] Krishnan I, Lee S. Effect of power factor correction circuit on switched reluctance motor drives for appliances. In: Applied Power Electronics Conference and Exposition, 1994. APEC '94. Conference Proceedings 1994., Ninth Annual; 13-17 Feb; Orlando, FL, USA: IEEE; 1994. p. 83-89. DOI: 10.1109/APEC.1994.316415

[18] Consoli A, Testa A, Aiello N, Gennaro F, Presti ML. Unipolar Converter for Switched Reluctance Motor Drives with Power Factor Improvement. In: APEC 2001. Sixteenth Annual IEEE Applied Power Electronics Conference and Exposition; 4–8 March; Anaheim, CA, USA: IEEE; 2001. p. 1103–1108. DOI: 10.1109/APEC.2001.912504

[19] Kwon YA, Shin JK, Rim GH. SRM Drive System with Improved Power Factor. In: Industrial Electronics, Control and Instrumentation, 1997. IECON 97. 23rd International Conference on; 14 Nov.; New Orleans, LA, USA: IEEE; 1997. p. 541–545. DOI: 10.1109/IECON.1997.671791

[20] Chai JY, Liaw CM. Development of a switched-reluctance motor drive with PFC front end. IEEE Transactions on Energy Conversion. 2009;**24**(1):30–42. DOI: 10.1109/TEC.2008.2002328

[21] Reinert J, Schroder S. Power-factor correction for switched reluctance drives. IEEE Transactions on Industrial Electronics. 2002;**49**(1):54–57. DOI: 10.1109/41.982248

[22] Goyal S, Kumar R, Gupta RA. Simulation and Analysis of Current Controlled PFC Converter-Inverter Fed SRM Drive. In: 2005 IEEE International Conference on Industrial Technology; 14–17 Dec; Hong Kong, China: IEEE; 2005. p. 1433–1437. DOI: 10.1109/ICIT.2005.1600860

[23] Kumar R, Gupta RA, Goyal S, Bishnoi SK. Fuzzy tuned PID controller based PFC converter-inverter fed SRM drive. In: 2006 IEEE International Conference on Industrial Technology; 2006. pp. 2498–2503. DOI: 10.1109/ICIT.2006.372632

[24] Rajesh M, Singh B. Power quality improvement in switched reluctance motor drive using Vienna rectifier. In: 2012 IEEE Fifth Power India Conference; 19–22 Dec; Murthal, India: IEEE; 2012. p. 1–7. DOI: 10.1109/PowerI.2012.6479580

[25] Rajesh M, Singh B. Analysis, design and control of single-phase three-level power factor correction rectifier fed switched reluctance motor drive. IET Power Electronics. 2014;**7** (6):1499–1508. DOI: 10.1049/iet-pel.2013.0621

[26] Chen YY, Hsu CT, Hu KW. On the PFC AC-DC Converter Fed SRM drives with Reversible and Regenerative Braking Capabilities. In: 2015 IEEE 2nd International Future Energy Electronics Conference (IFEEC); 1–4 Nov; Taipei, Taiwan: IEEE; 2015. p. 1–7. DOI: 10.1109/IFEEC.2015.7361545

[27] Singh B, Anand A. Improved Power Quality Zeta Converter Fed Switch Reluctance Motor Drive. In: 2015 2nd International Conference on Recent Advances in Engineering & Computational Sciences (RAECS); 21–22 Dec; Chandigarh, India: IEEE; 2015. p. 1–6. DOI: 10.1109/RAECS.2015.7453360

[28] Singh B, Anand A. A PFC Based SRM Motor Drive Using a Canonical Switching Cell Converter. In: 2016 IEEE 6th International Conference on Power Systems (ICPS); 4–6 March; New Delhi, India: IEEE; 2016. p. 1–6. DOI: 10.1109/ICPES.2016.7584246

[29] Chau KT. Switched Reluctance Motor Drives. In: Chau KT, editor. Electric Vehicle Machines and Drives: Design, Analysis and Application. 1st ed. eBook: Wiley-IEEE Press; 2015. p. 108–146. DOI: 10.1002/9781118752555.ch5

[30] Sehirli E, Kuyumcu FE, Cakir B. Current Controlled SRM fed by Three-phase Voltage Source Converter. In: 2015 50th International Universities Power Engineering Conference (UPEC); 1–4 Sept; Stoke on Trent, UK: IEEE; 2015. p. 1–6. DOI: 10.1109/UPEC.2015.7339858

[31] Singh B, Singh BN, Chandra A, Al-Haddad K, Pandey A, Kothari DP. A review of three-phase improved power quality AC-DC converters. IEEE Transactions on Industrial Electronics. 2004;**51**(3):641–660. DOI: 10.1109/TIE.2004.825341

[32] Sehirli E, Altınay M. Input-output linearization control of single-phase buck-boost power factor corrector. In: 2012 47th International Universities Power Engineering Conference (UPEC); 4–7 Sept; London, UK: IEEE; 2012. p. 1–6. DOI: 10.1109/UPEC.2012.6398557

[33] Slotine JJE, Li W. Applied Nonlinear Control. New Jersey: Prentice Hall; 1991

[34] Khalil HK. Nonlinear Systems. 3rd ed. New Jersey: Prentice Hall; 2002

[35] Lee TS. Input-output linearization and zero-dynamics control of three-phase AC/DC voltage-source converters. IEEE Transactions on Power Electronics. 2003;**18**(1):11–22. DOI: 10.1109/TPEL.2002.807145

[36] Kim CC, Hur J, Hyun DS. Simulation of a switched reluctance motors using Matlab/M-file. In: IEEE 2002 28th Annual Conference of the Industrial Electronics Society. IECON 02; 5–8 Nov; Sevilla, Spain: IEEE; 2002. p. 1066–1071. DOI: 10.1109/IECON.2002.1185420

[37] Huy LH/Mathworks. Switched Reluctance Motor [Internet]. Available from: https://www.mathworks.com/examples/simpower/mw/sps_product-power_SwitchedReluctanceMotor-switched-reluctance-motor [Accessed: March 2, 2017]